

Temperature-dependent current-conduction mechanisms in Au/n-InP Schottky barrier diodes (SBDs)

D. KORUCU^a, T.S. MAMMADOV^b

^aDepartment of Material Science and Engineering, Faculty of Engineering, Hakkari University, 38400, Hakkari -Turkey

^bPhysics Department, Faculty of Arts and Sciences, Gazi University, 06500, Ankara, Turkey

In this study, we have investigated the forward bias current-voltage (I - V) characteristics of Au/n-InP Schottky barrier diodes (SBDs) in the temperature range of 160-400 K. Experimental results show that the values of ideality factor (n), zero-bias barrier height $\Phi_{B0}(I$ - V) were found strongly temperature dependent and while the $\Phi_{B0}(I$ - V) increases, the n decreases with increasing temperature. Such behavior of $\Phi_{B0}(I$ - V) and n is attributed to Schottky barrier inhomogeneities by assuming a Gaussian distribution (GS) of barrier heights (BHs) at Au/n-InP interface. We attempted to draw a Φ_{B0} vs $q/2kT$ plot to obtain evidence of a GS of the BHs, and the values of $\bar{\Phi}_{B0}=0.89\text{eV}$ and $\sigma_{\sigma}=0.137\text{ V}$ for the mean barrier height and standard deviation at zero bias, respectively, have been obtained from this plot. Thus, a modified $\ln(I_0/T^2)-q^2\Phi_{B0}^2/2(kT)^2$ vs q/kT plot gives Φ_{B0} and Richardson constant A^* as 0.904 eV and $10.35\text{ A/cm}^2\text{K}^2$, respectively, without using the temperature coefficient of the barrier height. This value of the Richardson constant $10.35\text{ A/cm}^2\text{K}^2$ is very close to the theoretical value of $9.8\text{ A/cm}^2\text{K}^2$ for n-InP. Hence, it has been concluded that the temperature dependence of the forward I - V characteristics of the Au/n-InP SBDs can be successfully explained on the basis of TE mechanism with a Gaussian distribution of the BHs.

(Received January 23, 2011; accepted February 20, 2012)

Keywords: Au/InP contacts; MBE grown epilayer InP; Barrier inhomogeneities; Gaussian distribution, Temperature dependence

1. Introduction

Indium Phosphide (InP) is increasingly a promising material for high speed digital, optoelectronic and microwave applications, is also usefulness in radiation detector, semiconductor lasers, solar cells. Besides it has been reported that InP is more resistant to radiation as compared with Si and GaAs [1-5]. However one of the major problems on n -type InP for its application in electronic devices arises from a low metal- semiconductor barrier height which in turn leads to difficulty in making low leakage current Schottky diodes [6]. Also III-V semiconductor technology is faced with new difficulties respect to standard semiconductor such as Si and Ge. Unless specially fabricated, a SBD possesses a native insulator layer between metal/semiconductor (M/S) interfaces. The existence of such an insulator layer converts MS diodes into metal-insulator-semiconductor (MIS)-type diodes and raises the BH at M/S interface [7-9].

Analysis of the forward bias I - V characteristics of the SBD measured only at room temperature does not give detail information about the current-conduction mechanisms and nature of the BH formed MIS interface. On the other hand, when these measurements carried out at wide temperature range allow us to understand different aspects of current-conduction mechanism. Therefore, we have investigated the forward bias I - V characteristics of Au/n-InP (SBDs) in the temperature range of 160-400 K.

In this work, temperature dependent experimental analysis of the I - V data of SBD based on Thermoionic Emission (TE) theory usually exhibits an abnormal increase in barrier height BH Φ_{B0} and an decrease in the ideality factor n with a increase in the temperature which lead to non-linearity in the activation energy $\ln(I_0/T^2)$ vs. $1/T$ plot. Similar results have been reported in the literature [10-15]. The high values of ideality factor and barrier height can be ascribed to the existence of insulator layer at M/S interface, the image force lowering of the barrier and particular distribution of interface states at semiconductor band-gap [11,13-19]. Some researcher have been successfully explained the change in the BH and n with a changing temperature on the basis of a TE mechanism with a Gaussian distribution of the BHs [20-24]. The current transport mechanisms are dependent on several parameters such as inhomogeneity of the barrier height at M/S interface, surface preparation processes, insulator layer thickness at the metal/semiconductor interface, and density of interface states at insulator layer/semiconductor interface and series resistance of device [25-27]. Two main approaches have been proposed by Tung [12] and by Werner and Gütter [20] which assume a Gaussian distribution of the barrier height values on the metal/semiconductor interface. Also Werner and Gütter [20] assume a continuous spatial distribution of the BH, and the total current across a diode is obtained by integrating the TE current with an individual BH and weighted by using the GD function. According to this approach, the pinch-off effect related to the interaction

between adjacent regions with different barriers and the effective barrier are always lower than the mean value of the barrier distribution.

In this study, the forward bias current-voltage (I - V) characteristics of the Au/n-InP Schottky barrier diode have been examined in the temperature range of 160-400 K. The experimental analysis of the I - V - T in the temperature range of 160-400 K reveals an increase of BH but a decrease in n with increase in temperature. Such behavior of BH and n are interpreted based on the existence of Gaussian distribution (GD) of the BHs around a mean value due to BH inhomogeneities prevailing at the Au/n-InP. In addition, capacitance-voltage (C - V) measurement was performed at room temperature and 1 MHz.

2. Experimental procedure

In this study, Si doped n-type InP having thickness of 7000 \AA was grown on n-InP(100) substrate using the VG80H solid source molecular beam epitaxy (MBE) system. Before contact process, the n-InP wafer was dipped in $5 \text{ H}_2\text{SO}_4 + \text{H}_2\text{O}_2 + \text{H}_2\text{O}$ (1:1:300) solution for 1.0 min to remove surface damage layer and undesirable impurities and then in $\text{H}_2\text{O} + \text{HCl}$ solution and then followed by a rinse in de-ionized water. The wafer has been dried with high purity nitrogen (N_2) and inserted into the vacuum chamber immediately after the etching process then high purity gold (Au) metal (99.999%) with a thickness of 1020 \AA was thermally evaporated from the tungsten filament onto the whole back surface of the wafer in the pressure of $\sim 10^{-6}$ Torr. The ohmic contact was formed by sintering the evaporated Au contact at $400 \text{ }^\circ\text{C}$ for 90 min in flowing dry nitrogen ambient at a rate of ~ 2 l/min. After finishing this process, temperature was reduced to $300 \text{ }^\circ\text{C}$ and sample was annealed during 10 minutes. Then the sample was cooled to room temperature. To make Schottky contact on epilayer section, circular dot shaped Au Schottky contacts with a thickness of 1000 \AA were formed by evaporating Au in the pressure of $\sim 10^{-6}$ Torr. After this process Au/n-InP SBDs have been fabricated. Then the sample was removed from system and was soldered with silver pleat and then Schottky contacts were connected with conductor fiber by assistance of silver pleat. After fabrication of the Au/n-InP SBD, the current-voltage (I - V) characteristics have been measured in the temperature range of 160-400 K. C - V measurement has been carried out at room temperature in dark.

I - V and C - V measurements of Au/n-InP SBDs have been performed by using a Keithley 2400 Sourcemeter and a HP model 4192A LF impedance analyzer, respectively. I - V measurements have been carried out in the temperature range of 160-400 K using a temperature controlled Janes vpf-475 cryostat, which enables us to make measurements in the temperature range of 77-450 K. The bias voltage is swept from -1.5 to $+1.5$ V. The sample temperature was always monitored by use of a copper-constant thermocouple close to the sample and measured with a Keithley model 199 DMM/scanner and Lake Shore model

321 auto-tuning temperature controllers with sensitivity better than ± 0.1 K.

3. Results and discussions

3.1. Current-Voltage- Temperature (I - V - T) Characteristics

When the applied bias voltage $V > 3kT/q$, the forward bias current-voltage (I - V) relation according to thermionic emission (TE) theory for a Schottky barrier diode (SBD) with the series resistance can be written as follows when [25]

$$I = I_o \exp\left(\frac{q(V - IR_s)}{nkT}\right) \left[1 - \exp\left(-\frac{q(V - IR_s)}{kT}\right)\right] \quad (1)$$

where I_o is the reverse saturation current derived from the linear region of the intercept of $\ln I$ vs V at zero bias, and is given by Eq. (2), q is the electron charge, V is the voltage applied across the diode, IR_s is the voltage drop across the series resistance, k is the Boltzmann constant, T is the absolute temperature in K, R_s is the series resistance of diode, n is the ideality factor.

$$I_o = AA^* T^2 \exp\left(-\frac{q\Phi_{Bo}}{kT}\right) \quad (2)$$

where A is the rectifier contact area of the diode, A^* is the effective Richardson constant of $9.8 \text{ A/cm}^2\text{K}^{-2}$ for n-type InP [28] and Φ_{Bo} is the zero bias barrier height of the diode and their values were calculated from Eq.(2). From Eq. (1), ideality factor n can be written as

$$n = \frac{q}{kT} \left(\frac{dV}{d\ln I}\right) \quad (3)$$

Fig.1. shows the forward and reverse bias semi-logarithmic $\ln I$ - V characteristics of the Au/n-InP SBDs in the temperature range of 160-400 K. As seen in Fig.1, the $\ln I$ - V plots for each temperature give a straight line at high bias voltage region but it deviates considerably from linearity due to the effect of series resistance at high bias region. Also, the dark reverse current increases with increasing the applied reverse bias and does not show any effect of saturation. This lack of saturation for Au/n-InP SBD under reverse bias can be explained in the terms of the spatial inhomogeneity of BH [11,12], the existence of the insulator layer between metal and semiconductor and image force lowering in the barrier height. The other explanation of such behavior may be due to generation of electron-hole pairs in the depletion region as generation current is more pronounced at low temperatures than high temperatures [27-31].

The experimental values of Φ_{Bo} and n for the Au/n-InP SBD were determined from Eq. (2) and Eq. (3), respectively, and are given in Table 1 and Fig.2. As seen in Table 1, the values of Φ_{Bo} and n for the Au/n-InP SBD

ranged from 0.41eV and 1.82 (at 160 K) to 0.71eV and 1.35 (at 400 K), respectively. Such behavior of n was attributed to the existence of a thick insulator layer at metal/semiconductor interface and to particular distribution of interface states [14, 25, 32].

The ideality factors greater than unity are also ascribed to secondary mechanisms at the interface [33, 34]. As explained in refs. [17,21,35], since the current transport on the diode is a temperature-activated process carriers especially at low temperatures are able to surmount the lower barriers. Therefore the current conduction will be dominated by the current through the patches of lower SBH [14,17,18,25] and this situation will be lead to the increase of ideality factor. The possible mechanisms of current transport across the barrier are thermionic emission (TE), thermionic field emission (TFE), field emission (FE), recombination-generation, interface recombination tunneling, minority carrier injection, and multistep tunneling [25,27,36]. Which of these mechanisms dominate over others depends on the sample temperature, applied bias voltage, the formation of barrier height at M/S interface, the doping concentration, densities of surface states and series resistance of sample [36].

As can be seen in Table 1, the values of n are higher than unity for each temperature and decrease with increasing temperature. Also the values of n are not constant with temperature. The high values of the ideality factor show that there is a deviation from TE theory in the current conduction mechanism.

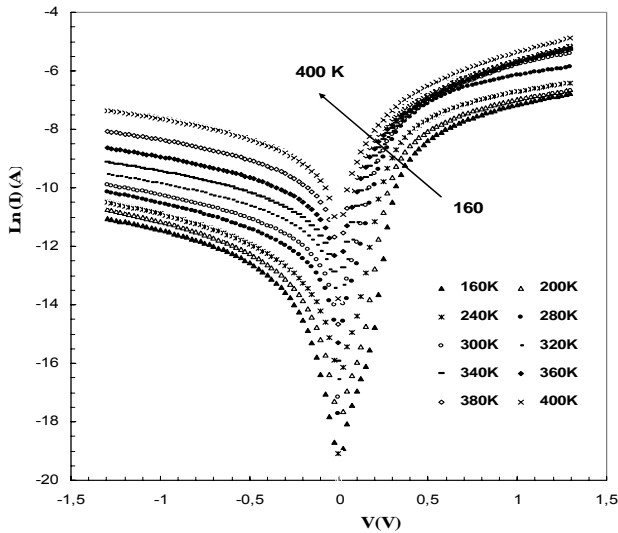


Fig.1. Temperature - dependent experimental forward and reverse bias semi-logarithmic current-voltage (I - V) characteristics of the Au/n-InP SBD.

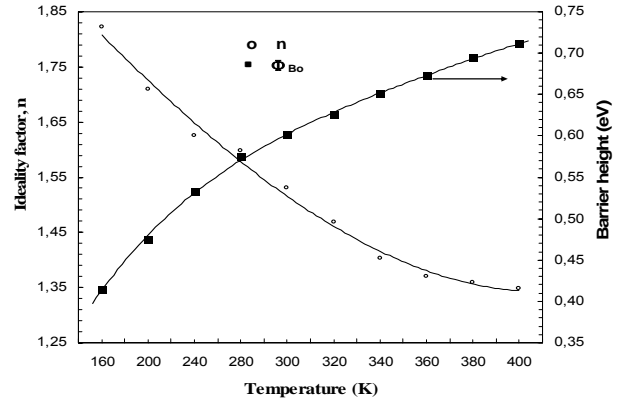


Fig. 2. Temperature dependent Φ_{B0} and n of the Au/n-InP SBD.

Moreover the ideality factor varies almost linearly with the inverse temperature (Fig. 3) as:

$$n(T) = n_o + T_o/T \quad (4)$$

where the n_o and T_o are constant which were found to be 1.04 and 131.52 K, respectively. In order to understand the dominant current transport mechanisms, the ideality factor is analyzed by plotting nkT/q vs. kT/q in Fig.4 which shows both the experimental and theoretical results of this plots. As shown in Fig 4, experimental and theoretical curves are linear and parallel. Such behavior of n is known as a T_o anomaly.

The thermionic field emission (TFE) theory requires a change in tunneling current parameter E_{oo} with temperature according to relation

$$E_o = n \frac{kT}{q} = E_{oo} \coth\left(\frac{qE_{oo}}{kT}\right) \quad (5)$$

where E_{oo} is the characteristic tunneling energy that is related to tunnel effect transmission probability as

$$E_{oo}(T) = \frac{h}{4\pi} \left(\frac{N_D(T)}{m_e^* \epsilon_{InP}} \right)^{\frac{1}{2}} = 1.85 \times 10^{-14} \left(\frac{N_D(T)}{m_e^* \epsilon_{InP}} \right)^{\frac{1}{2}} \text{ eV} \quad (6)$$

where $h=6.626 \times 10^{-34}$ J.s, in the case of our n-type InP, $N_D(T)$ value obtained from the slope of the linear plot of C^2 - V curve at 300 K (Fig. 8) is $4.63 \times 10^{22} \text{ m}^{-3}$, $m_e^* = 0.077 m_o$ (m_e^* is the effective mass of electron) and $\epsilon_{InP} = 12.56 \epsilon_o$ (ϵ_{InP} is the permittivity of InP), the corresponding E_{oo} values turn out to be 4.06 meV.

The FE mechanism becomes important when tunneling current parameter $E_{oo} \gg kT/q$ (E_{oo} is the characteristic tunneling energy), whereas, the TFE dominates when $E_{oo} \approx kT/q$. Therefore both the TFE and FE are unlikely current transport mechanisms. On the other hand, FE would predominate only at quite low temperatures and high doping concentrations, which is not the case for the InP substrate in the present study. Tunneling current can be important only highly doped semiconductor ($N_D \geq 1 \times 10^{17-18} \text{ cm}^{-3}$). In addition, the minority carrier diffusion is also unlikely mechanism for our sample in the intermediate bias region, since it would be expected to be significant only for the diode having very high effective BH value near to band gap of InP and very low reverse saturation current [25].

Table 1. Temperature dependent values of various parameters determine from forward bias I - V characteristics of the Au/n-InP SBD.

T (K)	I_o (A)	n	Φ_{Bo} (eV)
160	$1,71 \times 10^{-10}$	1,82	0,415
200	$3,33 \times 10^{-9}$	1,71	0,475
240	$2,86 \times 10^{-8}$	1,63	0,533
280	$2,77 \times 10^{-7}$	1,60	0,574
300	$5,46 \times 10^{-7}$	1,53	0,601
320	$1,08 \times 10^{-6}$	1,47	0,626
340	$1,98 \times 10^{-6}$	1,40	0,651
360	$3,76 \times 10^{-6}$	1,37	0,673
380	$6,66 \times 10^{-6}$	1,36	0,695
400	$1,37 \times 10^{-5}$	1,35	0,711

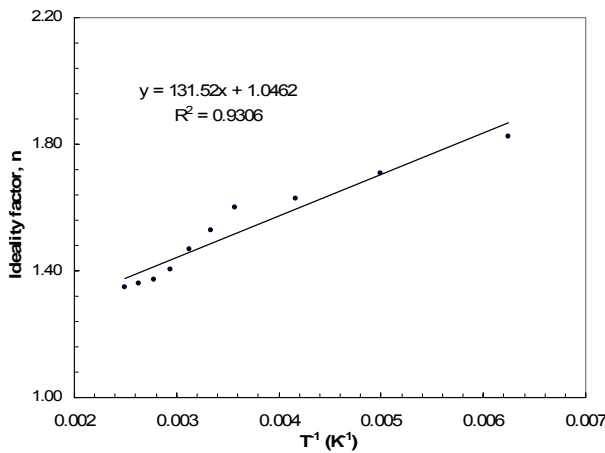


Fig. 3. n vs $1/T$ for Au/n-InP Schottky barrier diode.

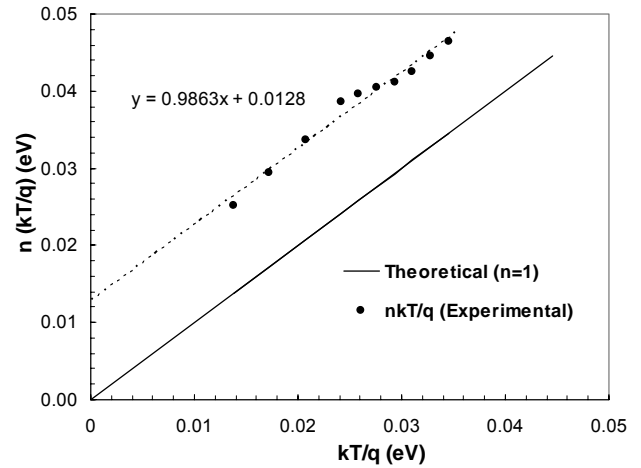


Fig. 4. The plot $E_o(=nkT/q)$ vs kT/q of the Au/n-InP SBD.

3.2 The Analysis of the Inhomogeneous Barrier and Modified Richardson Plot

In order to evaluate the BH, one might also use the conventional activation energy plot of the reverse saturation current I_o . Therefore, Eq. (2), can be rewritten as

$$\ln\left(\frac{I_o}{T^2}\right) = \ln(AA^*) - \frac{q\Phi_{Bo}}{kT} \quad (7)$$

Fig. 5 shows the Richardson plot of $\ln(I_o/T^2)$ vs $1/T$ and $\ln(I_o/T^2)$ vs $1/nT$ for the Au/n-InP SBD. Both of the plots were found to be linear in the measured temperature range. The values of activation energy (E_a) and Richardson constant (A^*) were obtained from the slope and intercept of this straight line of $\ln(I_o/T^2)$ vs $1/T$ as 0.217 eV and $3.87 \cdot 10^{-6} \text{ Acm}^{-2} \text{ K}^{-2}$, respectively, while in the $\ln(I_o/T^2)$ vs $1/nT$ plot the values of E_a and A^* were found as 0.52 eV and $5.68 \cdot 10^{-4} \text{ Acm}^{-2} \text{ K}^{-2}$, respectively. These A^* values are much lower than the known value of $9.8 \text{ Acm}^{-2} \text{ K}^{-2}$ for n-type InP [25]. In addition, especially the value of 0.217 eV obtained from the slope of $\ln(I_o/T^2)$ vs $1/T$ plot is lower than half of the energy band gap of InP. On the other hand the value of 0.52 eV obtained from the slope of $\ln(I_o/T^2)$ vs $1/nT$ plot is close to the half of the energy band gap of InP. These results confirm that the predominant current conduction mechanism is not only the TE.

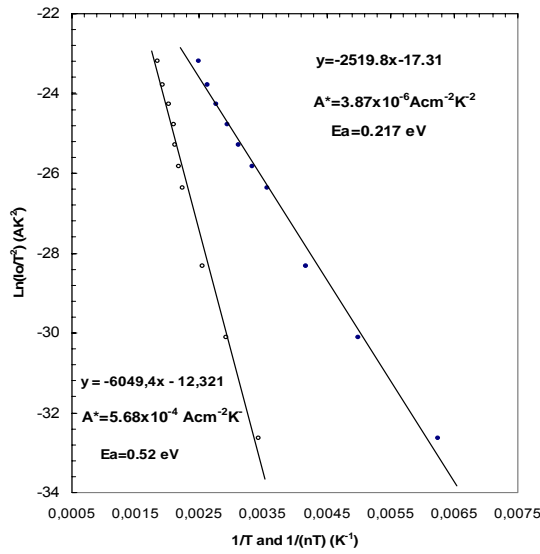


Fig.5. Richardson plots of the $\ln(I_o/T^2)$ vs $1/T$ or $1/nT$ for Au/n-InP SBD.

According to Tung's theoretical approach there is a linear correlation between the experimental zero bias BHs and ideality factors. Horvath [35] explained that the A^* value may be affected by the lateral inhomogeneity of the barrier. Also Song et al. [37] suggested that the contact area A is composed of many sub-areas, each having a definite BH and a definite area a being isolated from each other. They show that in Schottky barrier (SB) contacts variations of the BH over the contact area can occur as a result of inhomogeneities in the interfacial oxide layer composition, non-uniformity of the interfacial layer thickness and distributions of interfacial charges. Fig.6 shows a plot of experimental Φ_{B_0} vs n for various temperature. As can be seen in Fig.6, there is a linear relationship between the Φ_{B_0} and n that was explained by lateral inhomogeneities of the BHs in the Au/n-InP SBD. The extrapolation of the Φ_{B_0} vs n plot to $n=1$ has given a homogeneous BH of approximately 0.905 eV. Thus it can be said that the significant decrease of the zero-bias BH and increase of n especially at low temperature are possibly caused by the BH inhomogeneities.

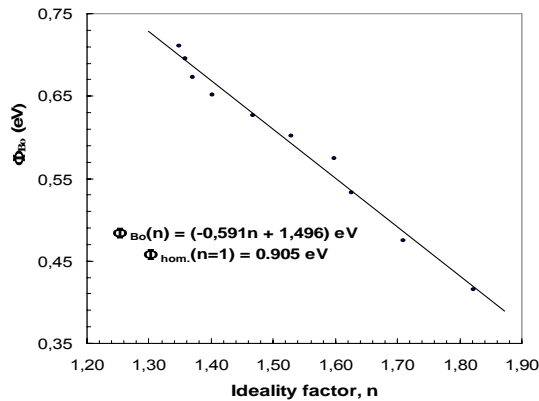


Fig.6. Temperature-dependent experimental Φ_{B_0} vs. n plot of the Au/n-InP SBD.

The Gaussian distribution of the BHs with a mean value $\bar{\Phi}_{B_0}$ and standard deviation σ_o yields the following expression of the BH as [16,19,37]

$$\Phi_{ap} = \bar{\Phi}_{B_0}(T=0) - \frac{q\sigma_o^2}{2kT} \quad (8)$$

where the temperature dependence of σ_o is usually small and can be neglected [14,17,38]. The observed variation of ideality factor with temperature in the model is given by [11,13, 18-20]

$$\left(\frac{1}{n_{ap}} - 1 \right) = \rho_2 - \frac{q\rho_3}{2kT} \quad (9)$$

where n_{ap} is apparent ideality factor and ρ_2 and ρ_3 are voltage coefficients, which may depend on temperature, quantifying the voltage deformation of the BH distribution [13,39,40].

The experimental Φ_{B_0} vs $q/2kT$ and n_{ap} vs $q/2kT$ plots in Fig. 7 were drawn to obtain evidence of a GD [10-16] of BHs. Thus, the plot of Φ_{ap} vs $q/2kT$ (Fig.7) should be a straight line that with the intercept at the ordinate determining the zero-bias mean BH $\bar{\Phi}_{B_0}(T=0) = 0.89$ eV and a slope giving the standard deviation $\sigma_o = 0.137$ V. It was seen that the value of $\sigma_o = 0.137$ V is not small compared to the mean value of $\bar{\Phi}_{B_0} = 0.89$ eV, indicating the presence of the interface inhomogeneities. Similarly, as can be seen from Fig.7, the value of ρ_2 obtained from the intercept of the experimental n_{ap} vs $q/2kT$ plot is -0.1426 and the value of ρ_3 from the slope is -0.092 V. These results indicate that the presence of single GD BHs in the Schottky contact area.

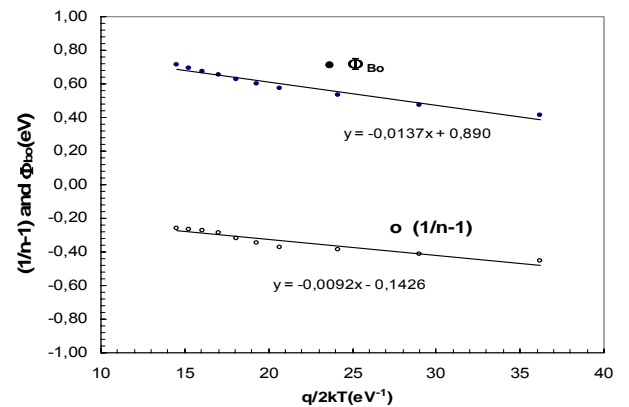


Fig.7. Φ_{B_0} (I - V) and $(1/n-1)$ vs $q/2kT$ plots for Au/n-InP SBD according to GD of barrier heights.

Furthermore, as indicated above, the conventional activation energy $\ln(I_0/T^2)$ vs q/kT plot, to explain these behaviors, the combination of Eqs. (2) and (8) according to GD of the BH, the modified Richardson plot can be rewritten as

$$\ln\left(\frac{I_0}{T^2}\right) - \left(\frac{q^2 \sigma_o^2}{2k^2 T^2}\right) = \ln(AA^*) - \frac{q\bar{\Phi}_{B0}}{kT} \quad (10)$$

As can be seen in Fig. 8, modified $\ln(I_0/T^2) - q^2 \sigma_o^2 / 2k^2 T^2$ vs q/kT plot according to Eq.(10) should give a straight line with the slope directly yielding the mean barrier height $\bar{\Phi}_{B0}$ and the intercept ($=\ln AA^*$) at the ordinate determining A^* for a given diode area A . The values of $\bar{\Phi}_{B0}$ and A^* were obtained as 0.904 eV and $10.35 \text{ Acm}^{-2} \text{ K}^{-2}$, respectively, without using the temperature coefficient of the BHs. Interestingly, the value of A^* is in reasonable agreement with the theoretical value of $9.8A \text{ cm}^{-2} \text{ K}^{-2}$ for electrons in n -type InP. Also, the value of $\bar{\Phi}_{B0} = 0.90 \text{ eV}$ from this plot is in close agreement with the value of $\bar{\Phi}_{B0} = 0.89 \text{ eV}$ from the plot of Φ_{ap} vs $q/2kT$. Hence, it has been concluded that the forward bias I - V characteristics of Au/n-InP Schottky barrier diode can be successfully explained on the basis of TE theory with a GD of the BHs.

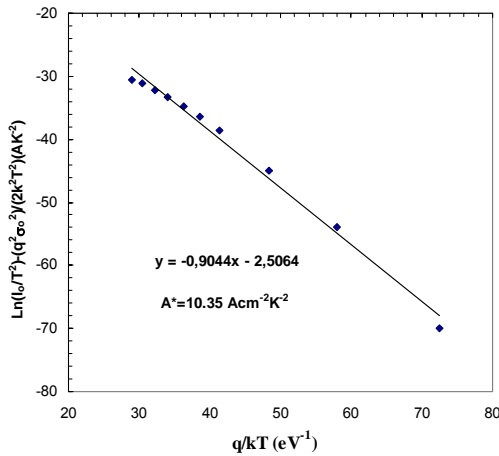


Fig. 8. Temperature dependence of $\ln(I_0/T^2) - ((q\sigma_o)^2 / (2k^2 T^2))$ vs q/kT for Au/n-InP SBD.

3.3. Capacitance-Voltage (C-V) Characteristics at Room Temperature

The measured capacitance-voltage (C - V) and C^{-2} vs V at 1 MHz for Au/n-InP SBD are shown in Fig. 9 at the room temperature. When the measurements are carried out at high frequency ($f \geq 1 \text{ MHz}$) the charge at the interface states cannot follow an ac signal [25,41]. Therefore, the C - V measurement was performed at 1 MHz. As can be seen

in Fig. 9, the value of capacitance gives the peak at forward bias about 0.2 V bias. We think that the series resistance and surface states of the SBD are responsible for such anomalous peak in the forward bias. When a small ac voltage of a few mV is applied to a reverse biased diode the depletion region capacitance C is given by a relation

$$C^{-2} = \frac{2}{q\epsilon_s A^2 N_D} (V_o + V) \quad (11)$$

where A is the area of the diode, ϵ_s is the permittivity of semiconductor, N_D is the carrier doping density of donors, V is the magnitude of the applied bias and V_o is the intercept of C^{-2} with the voltage axis and is given by

$$V_o = V_D + kT/q \quad (12)$$

As shown in Fig. 9, the C^{-2} - V plots at 1 MHz are linear lines at wide voltage. The linear plot C^{-2} - V is very useful for analyzing the experimental C - V characteristics. Thus, the value of barrier was obtained from Fig. 9 as

$$\Phi_B(C-V) = V_o + kT/q + E_F = V_D + E_F \quad (13)$$

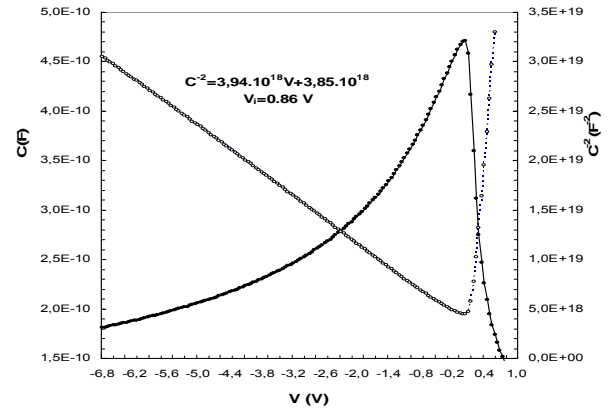


Fig. 9. Plots of forward and reverse bias C vs V and C^{-2} vs V of the Au/n-InP SBD at room temperature.

where V_D is the diffusion potential and E_F is the energy difference between the Fermi level and conduction band edge, and obtained $N_c = 4.82 \times 10^{15} T^{3/2} (m_e^* / m_o)^{3/2}$ with $(m_e^* / m_o) = 0,077$

$$E_F = \frac{kT}{q} \ln(N_D / N_c) \quad (14)$$

Here, N_c is the effective density of states in the InP conduction band, m_e^* is the effective mass of electrons and m_o is the rest mass of the electron. Thus, the values of N_D , E_F and Φ_B (C - V) were obtained from the reverse bias

C^{-2} - V plot as $4.63 \times 10^{22} \text{ m}^{-3}$, 0.135 eV and 1.02 eV, respectively. This value of $\Phi_{Bo}(C-V)$ obtained from the reverse bias $C-V$ measurement is greater than the value of $\Phi_{Bo}(I-V)$ obtained from forward bias $I-V$ measurement at room temperature and this discrepancy can be attributed to the natural of $I-V$ and $C-V$ measurement techniques. Song et. al [37] have shown that an inhomogeneous barrier also leads to a $\Phi_{Bo}(I-V)$ and $\Phi_{Bo}(C-V)$ difference. This discrepancy could be explained due to an interfacial layer or trap states in the semiconductor, the tunneling through the barrier top, the effect of the image force and the existence of Schottky barrier height inhomogeneity [16, 20, 37].

4. Conclusions

The forward bias $I-V$ characteristics of the Au/n-InP Schottky barrier diodes were measured in the temperature range of 160-400 K. Using the evaluation of the experimental forward bias I-V characteristics based on TE mechanism reveals an increase of Φ_{Bo} and a decrease of the ideality factor with increasing temperature. It is clear that such behavior of $\Phi_{Bo}(I-V)$ is an obvious disagreement with the reported negative temperature coefficient of the barrier height (BH). Such behavior of $\Phi_{Bo}(I-V)$ and n is attributed to Schottky barrier inhomogeneities by assuming a Gaussian distribution of barrier heights (BHs) due to barrier inhomogeneities that prevails at M/S interface. Therefore, we attempted to draw a Φ_{Bo} vs $q/2kT$ plot to obtain evidence of a GS of the BHs, and the values of $\bar{\Phi}_{Bo}=0.89 \text{ eV}$ and $\sigma_{\phi}=0.137 \text{ V}$ for the mean barrier height and standard deviation at zero bias, respectively, have been obtained from this plot. Thus, a modified $\ln(I_0/T^2) - q^2 \sigma_{\phi}^2 / 2(kT)^2$ vs q/kT plot gives $\bar{\Phi}_{Bo}$ and Richardson constant A^* as 0.904 eV and $10.35 \text{ A/cm}^2\text{K}^2$, respectively. This value of the Richardson constant $10.35 \text{ A/cm}^2\text{K}^2$ is very close to the theoretical value of $9.8 \text{ A.cm}^{-2}\text{K}^{-2}$ for n-InP. In summary, the temperature dependence of the forward I-V characteristics of the Au/n-InP SBDs can be successfully explained on the basis of TE mechanism with a Gaussian distribution of the BHs.

Acknowledgments

This work is supported by DPT2001 K120590 and Gazi University BAP research projects 05/2008-23.

References

- [1] C.H. Kim, Y. Jeong, T. Kim, S. Choi, K. Yang, J. Semicond. Technol. Sci. **6**, 154 (2006).
- [2] Y.-S. Lin, J.-H. Huang, J. Electrochem. Soc. **152**, G627 (2005).
- [3] A. Khan, Solid-State Electron **44**, 639 (2000).
- [4] M. Yamaguchi, C. Uemura, A. Yamamoto, J Appl. Phys. **55**, 1429 (1984).
- [5] K. Ando, M. Yamaguchi, Appl. Phys. Lett. **47**, 846 (1985).
- [6] O. Wada, A. Majerfeld, Electron. Lett. **14**, 755 (1978).
- [7] Z. Benamara, B. Akkal, A. Talbi, B. Gruzza, L. Bideux, Materials Science and Engineering C **21**, 287 (2002).
- [8] B. Akkal, Z. Benamara, A. Boudissa, N. B. Bouiadjra, M. Amrani, L. Bideux, B. Gruzza, Materials Science and Engineering **B55**, 162 (1998).
- [9] B. Akkal, Z. Benamara, L. Bideux, B. Gruzza, Microelectronics Journal **30**, 673 (1999).
- [10] P. Cova, A. Singh. Solid-State Electron **33**(1), 11 (1990).
- [11] J. P. Sullivan, R. T. Tung, M. R. Pinto, W. R. Graham, J. Appl. Phys. **70**, 7403 (1991).
- [12] R.T. Tung, Mat. Sci. Eng. R **35**, 1 (2001).
- [13] A. Gümüş, A. Türüt, N. Yalçın, J. Appl. Phys. **91**, 245 (2002).
- [14] S. Zeyrek, Ş. Altındal, H. Yüzer, M. M. Bülbül, Appl. Surf. Sci. **252**, 2999 (2006).
- [15] D. Korucu, Ş. Altındal, T. S. Mammadov, S. Özçelik, Optoelectron. Adv. Mater.– RC **2**, 525 (2008).
- [16] J.H. Werner, H.H. Güttler, J. Appl. Phys. **69**, 1522 (1991).
- [17] Ş. Karataş, Ş. Altındal, A. Türüt, A. Özmen, Appl. Surf. Sci. **217**, 250 (2003).
- [18] F. Lucolano, F. Roccaforte, F. Giannazzo, V. Raineri, J. Appl. Phys. **102**, 113701 (2007).
- [19] S. Chand, S. Bala, Appl. Surf. Sci. **252**, 358 (2005).
- [20] M. Biber, M. Cakar, A. Turut, J. Materials in Electron. **12**, 575 (2001).
- [21] S. Chand, J. Kumar, Semicond. Sci. Technol. **11**(1), 1203 (1996).
- [22] S. Chand, J. Kumar, Appl. Phys. A. **65**, 497 (1997).
- [23] S. Bandyopadhyay, A. Bhattacharyya, S.K. Sen, J. Appl. Phys. **85**, 3671 (1999).
- [24] S. Zhu, R.L. Van Meirhaeghe, C. Detavernier, F. Cardon, G.P. Ru, X.P. Qu, B.Z. Li, Solid-State Electron. **44**, 663 (2000).
- [25] S.M. Sze, Physics Semiconductor Devices, John Wiley and Sons, New York, 1981.
- [26] H.C. Card, E.H. Rhoderick. J Phys D: Appl Phys. **4**, 1589 (1971).
- [27] E.H. Rhoderick, R.H. Williams, Metal Semiconductor Contacts. 2nd Ed. Oxford, Clarendon Press, (1988).
- [28] R.H. Williams and G.Y. Robinson Physics and Chemistry of III-V Compound Semiconductor Interfaces, Edited by C.W. Wilmsen, (Plenum Press, New York 1985).
- [29] S.R. Forest, M.L. Kaplan, P.H. Schmidt, J. Appl. Phys. **55**, 1492 (1984).
- [30] P. Chattopadhyaya, A.N. Daw, Solid-State Electron. **29**, 55 (1986).
- [31] T.U. Kampen, W. Mönch, Surf. Sci. **331-333**, 490 (1995).
- [32] Ş. Altındal, İ. Dökme, M.M. Bülbül, N. Yalçın, T. Serin, Microelectron. Eng. **83**, 499 (2006).

- [33] S. Chand, S. Bala, *Physica B* **390**, 179 (2007).
- [34] W. Mönch, *J. Vac. Sci. Tech. B.* **17**, 1867 (1999).
- [35] Zs.J. Horvarth, *Solid-State Electron.* **39**, 176 (1996).
- [36] S.Varma, K.V. Rao, and S.Kar, *J.Appl.Phys.* **56**, 2812 (1984).
- [37] Y.P. Song, R.L. Van Meirhaeghe, W.H. Laflere, F. Cardon, *Solid-State Electron.* **29**, 663 (1986).
- [38] M.K. Hudait, P. Venkateswarlu, S.B. Krupanidhi, *Solid-State Electron.* **45**, 133 (2001).
- [39] S. Zhu, R.L. Van Meirhaeghe, C. Detavernier, F. Cardon, G.P. Ru, X.P. Qu, B.Z. Li, *Solid-State Electron.* **44**, 663 (2000).
- [40] S. Zhu, C. Detavernier, R.L. Van Meirhaeghe, F. Cardon, G.P. Ru, X. P. Qu, B.Z. Li, *Solid-State Electron.* **44**, 1807 (2000).
- [41] E.H. Nicollian, J.R. Brews, *MOS (metal oxide semiconductor) Physics and Technology*, Wiley, New York (1982).

*Corresponding author: dkorucu@yahoo.com